Biomedical Microdevices (2019) 21:85
https://doi.org/10.1007/s10544-019-0429-2

Microfabricated calorimeters for thermometric enzyme linked immunosorbent assay in one-Nanoliter droplets

Brad Lubbers[1] · Evan Kazura[1] · Elliott Dawson[2] · Ray Mernaugh[3] · Franz Baudenbacher[1]

Abstract
Advances in microfabrication allow for highly sensitive calorimeters with dramatically reduced volume, decreased response time and increased energy resolution. These calorimeters hold the potential for designs of ELISA platforms competitive with fluorescent and chemiluminescent technologies. We have developed a new assay platform using conventional ELISA reagents to produce a thermal signal quantifiable using calorimetry. Our optimized micromachined calorimeters have nL reaction volumes and a minimum detectable power of 375 pW/Hz$^{1/2}$. We demonstrate rapid quantification in a model system of trastuzumab, a humanized monoclonal antibody used in the treatment of HER2 overexpressing breast cancers, in human serum using a HER2 peptide mimetic. Trastuzumab concentration and reaction time constant correlated well ($R^2 = 0.954$) and can be used to determine trastuzumab concentrations. The limit of detection for the ThermometricELISA (TELISA) was 10 μg/ml trastuzumab in human serum. TELISA allows for a simple readout, reduction in assay time, sample and reagent volumes and has the potential to become a point of care multiplexed platform technology.

Keywords Calorimeter · Biosensor · ELISA · ThermometricELISA · Trastuzumab

1 Introduction

Therapeutic monoclonal antibodies (mAbs) are of particular interest as an emerging alternative to small-molecule drugs for the treatment of conditions such as cancer, infections, cardiovascular disease, and immune disorders (Piggee 2008) (Dolgova et al. 2014). The first mAb approved for solid tumor cancer treatment, trastuzumab (Herceptin®, Genentech USA), is a humanized IgG1κ useful against HER2 positive breast cancers (Esteva et al. 2002). However, in some patients, cellular Fc receptors responsible for binding to and recycling trastuzumab are atypical; and as such, trastuzumab is cleared quicker from the body resulting in reduced therapeutic efficacy (Pohlmann et al. 2009). In order to improve patient outcome and limit high cost treatment courses, serum titer measurements can be used to determine patient trastuzumab clearance rates and appropriate dosages for efficient treatment. The most abundant class/subclass of antibody present in human serum is IgG1 and normally ranges in concentration from 9 to 12 mg/ml of serum (Delves and Roitt 2011). Trastuzumab is a genetically engineered humanized IgG1 kappa light chain mAb, however since it incorporates human IgG1 constant domains it is difficult to distinguish from normal human antibodies (Morell et al. 1971). To overcome this, Jiang et al. used phage display to select for the HER2 peptide mimotope (designated Ch-19, sequence: CGSGSGSQLGPYELWELSH) that trastuzumab binds (Jiang et al. 2005). Another phage displayed recombinant antibody (2B4 scFv) has been successfully immobilized onto a gold sensor surface for use in a piezoimmunosensor (i.e. quartz crystal microbalance) assay to capture and detect trastuzumab present in solution (Shang et al. 2012).

Enzyme linked immunosorbent assays (ELISAs) have become the gold standard for measuring antibodies and antigens, both native and introduced, in biological samples (Premjeet et al. 2011) since the 1970s. Of the many commercially available microtiter-based ELISA kits, most utilize an enzyme linked to a detecting antibody to produce a colorimetric, chemiluminescent, or fluorescent signal that can be quantified using a microtiter plate reader. The need to increase sensitivity and reduce sample consumption and assay time drives research toward a rapid, low-volume, direct readout ELISA system (Ng et al. 2010).

✉ Franz Baudenbacher
F.Baudenbacher@vanderbilt.edu

[1] Department of Biomedical Engineering, Vanderbilt University, PMB 351631, 2301 Vanderbilt Place, Nashville, TN 37235-1631, USA

[2] BioVentures, Inc., 1435 Kensington Square Court, P.O. Box 2561, Murfreesboro, TN 37133-2561, USA

[3] Vanderbilt University School of Medicine, PRB 895, Nashville, TN 37232, USA

Published online: 27 August 2019

The most frequent substrate in ELISA is hydrogen peroxide, which is catalytically reduced by horseradish peroxidase (HRP, EC 1.11.1.7). The reaction enthalpy associated with the decomposition of H_2O_2 is large (−98 kJ/mol) making it an attractive target for calorimetric determination. Mattiasson et al. was the first to create an ELISA system with a calorimetric readout, termed Thermometric Enzyme Linked Immunosorbent Assay (TELISA). The original TELISA system was based on inhibition binding of a catalase linked albumin to an antibody coated calorimetry column (Mattiasson et al. 1977). These flow through systems required a large sample volume (>0.5 ml) and the use of temperature controlled thermistor columns, but sensitivity to the μg/ml level for insulin, human IgG, and albumin were achieved (Lammers and Scheper 1999). However, in the years following, fluorescent and chemiluminescent ELISA systems achieved much higher sensitivity, so TELISA has seen little use in the past decade.

Advances in microfabrication allow for highly sensitive calorimeters with dramatically reduced volume, which decreases response time and increases energy resolution. These calorimeters hold the potential for designs of TELISA systems competitive with fluorescent and chemiluminescent ELISAs. Previous calorimeters based on off-the-shelf thin film IR sensors showed a minimum energy resolution of 1.5 nW/Hz$^{1/2}$ and suffered from evaporative droplet loss (Lubbers and Baudenbacher 2011). The Zuo group used a polyimide film and PDMS chamber to minimize heat conduction and sample evaporation in a vanadium oxide thermistor-based calorimeter, but suffer from time constants of several seconds (Wang et al. 2017). Other micro-calorimeter designs utilize a Si based membrane or quasi 2-D microfluidic flow channels that decrease heat flow and result in minimum power sensitivity of several nanowatts (Carreto-Vazquez et al. 2011) (Feng et al. 2018) (Johannessen et al. 2002) (Verhaegen et al. 2000). Previous micro-calorimeter designs have utilized materials like gold and nickel that are easy to fabricate and have low resistance, but lack the high Seebeck coefficient needed for high sensitivity (Johannessen et al. 2002) (Lee et al. 2009). Therefore, new calorimeters were designed to incorporate high Seebeck coefficient materials in the thermopile, a low thermal conductivity polymer membrane, better vapor sealing, and optimized geometries.

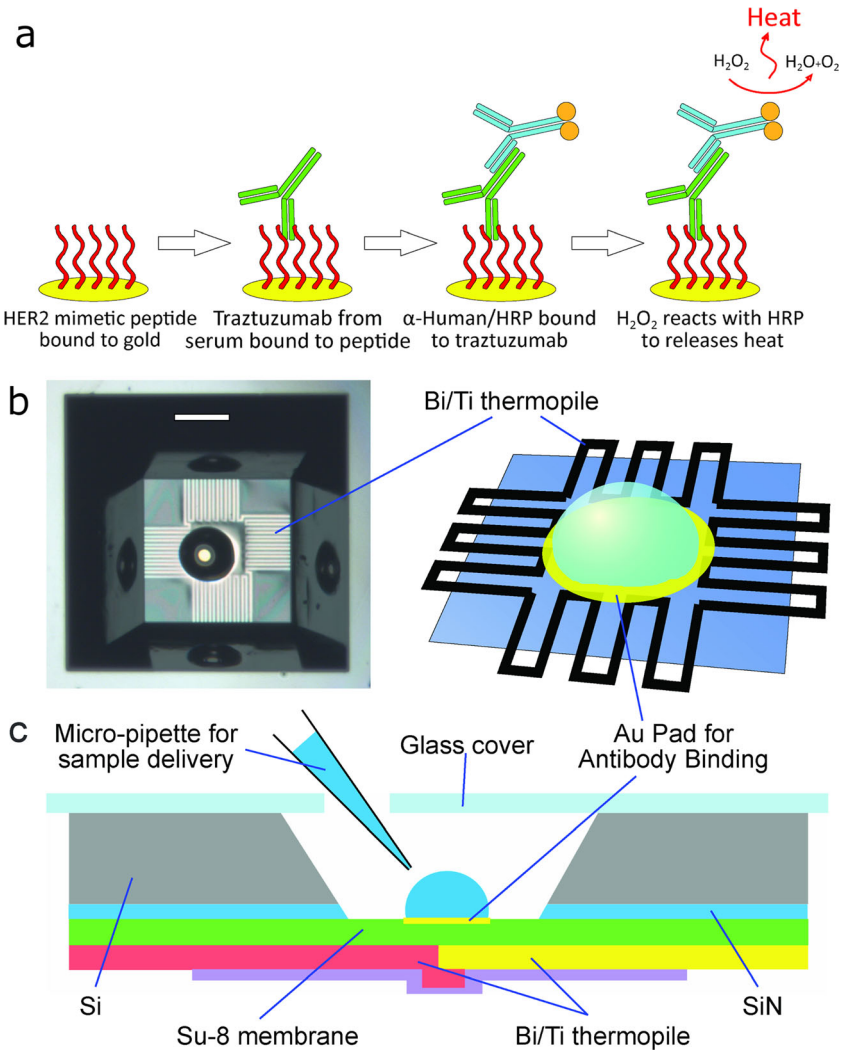

Fig. 1 TELISA steps. **a** The binding steps of the TELISA follow that of a traditional sandwich ELISA. However, in the detection step, the heat from the reaction of H2O2 and OPD with HRP is quantified, rather than a chromogenic or fluorescent measurement. All steps can be carried out in a 1-nanoliter volume, greatly reducing reagent and sample consumption. **b** A 1 nl sample drop sits atop a suspended Su-8 membrane on which a 28 Bi/Ti thermopile junction has been patterned. The Su-8 membrane and gold pad are used to immobilize the HER2 peptide mimetic, confine the sample droplet, and carry out the reaction for trastuzumab detection. Scale bar 200 μm. **c** The sample drop sits in an anisotropically etched Si pit and is accessed through a hole in the cover via a glass micropipette

Here, we report utilization of a micromachined calorimeter for a sandwich based thermal ELISA with nanoliter sample volumes. Figure 1a shows the ELISA construct, antibody binding steps, and the thermal readout step with HRP. Since a known amount of energy is released when a finite substrate supply is consumed, the area under the curve is preserved. The time course then indicates the amount of enzyme present. Furthermore, reduction of the sample volume maximizes the surface area to volume ratio to increase assay sensitivity. By operating in a 1 nl reaction volume, antibody and sample consumption is also greatly diminished. This has the added benefit of minimizing antibody binding time by reducing diffusion distance, such that a multi-step sandwich ELISA can be performed in less than 5 min (Kudo et al. 2008). This allows for the potential of pinprick point of care measurements that incorporate on-chip microfluidics to automate sample handling. Since many commercial ELISA systems already rely on a peroxidase/peroxide reporter system, many off-the-shelf kits can be converted for use in TELISA. Significant advantages of the TELISA over traditional ELISAs are a reduction in assay times, conservation of sample volume, and direct readout.

2 Materials and methods

2.1 Device design

Since the energies involved in the enzymatic reactions of ELISA in nanoliter volumes can be quite small (< 100 nJ) and over a time period greater than 100 s, a highly sensitive calorimeter capable of sub-nanowatt resolution is needed. In order to maximize sensitivity, our microcalorimeter features a small working volume, low thermal conductivity membrane, and materials with a high absolute Seebeck coefficient (Fig. 1b-c). The ideal calorimeter would have a very wide membrane on which the reaction droplet and thermopile sit to minimize thermal conduction away from the droplet. However, this creates long thermopile tracks with high electrical resistance. This leads to an increase in Johnson noise, the limiting factor in minimum detectable power. Since the resistance and thermoelectric properties of thin film metals can vary greatly from the bulk properties (Boyer and Cissé 1992), we performed four point sheet resistance and thermoelectric measurement of various metals to find those most suitable for our calorimeter. Material pairs were evaluated on experimentally found Seebeck coefficient (S) and electrical resistivity (ρ), as well as literature thermal conductivity (κ) in a figure of merit Z*.

$$Z^* = \frac{S}{0.25\kappa + \sqrt{\rho}}$$

Table 1 Figure of merit for potential thermopile materials. Bismuth and titanium (bold) combined the best Z* with ease of patterning. (Lubbers 2015)

	Z*	thin film Z*
Bi/Sb	3.446	2.517
Ni/Au	0.337	0.288
Ni/Ti	0.900	0.644
Ni/Cr	1.097	0.680
Bi/Ti	**2.447**	**1.682**
Bi/Cr	2.288	1.516
Bi/NiCr	2.421	1.754

Results for metal pairs we had the capability to deposit and pattern are shown in Table 1. A full description of material properties and the process can be found in Lubbers 2015. Bismuth and antimony provided the best combination of high conductivity and high absolute Seebeck coefficient, but proved difficult to pattern in thin traces together. Bi/chromium and Bi/nichrome both form a rough surface with high resistance when deposited over Su-8. Therefore, bismuth and titanium proved to be the best combination of Z* and ease of patterning.

A COMSOL Multiphysics/ MATLAB model was built based on previous calorimeter designs (Lubbers and Baudenbacher 2011). Variables were introduced to change the sensing area and membrane size while maximizing sensitivity and minimizing thermopile resistance. An iterative approach showed for a 1 nl drop, the optimal calorimeter had a membrane width of 525 μm and a sensing area width of 200 μm with 28 junctions. 1 nl was chosen as the optimal drop size as previous work had shown that as drop volume decreases, sensitivity increases, but must be balanced with sample evaporation to allow sufficient measurement time (Lubbers and Baudenbacher 2011). Variables for thermopile thickness were also introduced and it was found that a Ti thickness of 200 nm and a Bi thickness of 400 nm provided the best balance of thermal and electrical conductivity.

2.2 Device fabrication

All micromachining was performed in the cleanrooms at Vanderbilt University. 75 mm diameter silicon wafers, <100> orientation, double side polished, with 500 nm low stress silicon nitride (SiN) coated on both sides were obtained from WRS Materials (San Jose, CA). Chrome on soda-lime photomasks were produced by Advance Reproductions Corp. (North Andover, MA). Photoresist and developer were procured from MicroChem Corp. (Westborough, MA). All other chemical were from Fisher Scientific (Pittsburgh, PA). The microfabrication steps are displayed in Fig. 2. Pits are etched anisotropically in the silicon substrate, revealing a sacrificial silicon nitride membrane. An Su-8 polymer membrane is applied to the untouched side of the wafer, forming a base on which to construct the microcalorimeter. Titanium and

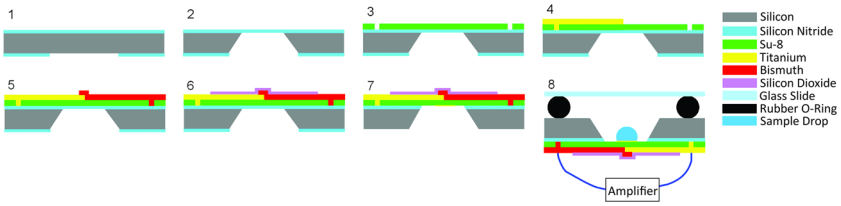

Fig. 2 Microcalorimeter microfabrication steps. (1–2) Anisotropically etched pit is formed in the silicon substrate, revealing a sacrificial silicon nitride membrane. (3) Su-8 polymer membrane is applied. (4–5) Bismuth and titanium thermopile tracks are deposited and patterned. (6) Silicon dioxide passivation layer is applied. (7) The remaining silicon nitrite under the membrane is removed and the gold binding spot applied. (8) The finished device is paired with a glass lid and o-ring to prevent sample evaporation and attached to a low noise amplifier during measurements

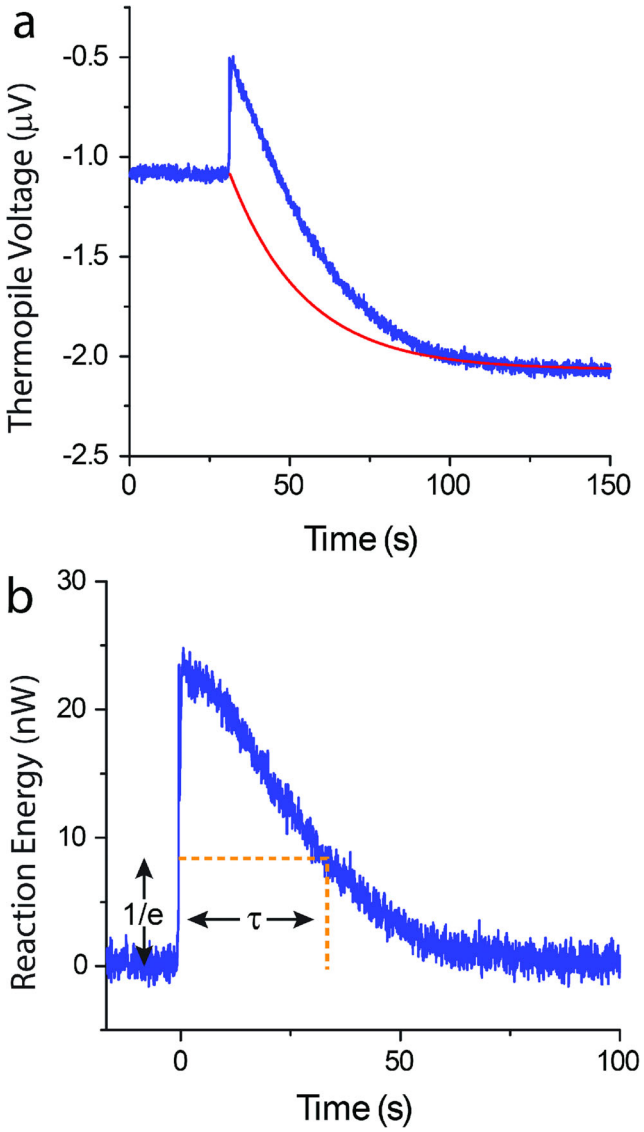

Fig. 3 Baseline correction and τ calculation (**a**) Uncorrected thermopile output voltage from TELISA detection of 50 μg/ml trastuzumab in human serum. The negative offset after peroxide injection is due to changes in the evaporation rate of the sample droplet. An exponential (red line) is fit to the curve so that the offset can be removed. **b** After the offset is removed, voltage can be converted to heat energy based on calorimeter sensitivity (45 *V*/*W*). The 1/e decay time (τ) of the signal is used to determine trastuzumab concentration

bismuth thermopile tracks are deposited by e-beam thermal deposition and patterned by hydrofluoric acid chemical etch and ion milling, respectively. Silicon dioxide passivation layer is applied for electrical isolation of the thermopiles. Reactive ion etching removes the remaining silicon nitrite under the membrane, freeing the thermally-isolated sensing areas of the microcalorimeters. Finally, gold contact pads are deposited by e-beam thermal evaporation through a shadow mask.

2.3 Device operation

Reaction chamber was formed by securing a rubber o-ring to the chip surface around the microcalorimeter sensing area. Device was attached to a custom, low-noise, DC chopper amplifier. The reaction chamber was then sealed with mineral oil and a glass slide. Liquid samples were delivered via an air driven Picospritzer II (Parker Hannifin, Cleveland, OH) using a glass micropipette positioned by a micromanipulator (MP-285, Sutter Instrument Co, Novato, CA). Access to the device was achieved through a hole drilled in glass slide and sealed with mineral oil to prevent sample evaporation. As reaction occurred on the calorimeter, voltage from thermopiles was recorded in LabView over time. Once reaction reached equilibrium, recording was stopped. Microcalorimeter devices can be reused by rinsing the sample well with toluene to remove any manufacturing residue or protein left from previous tests.

2.4 Materials

In this study, we used Ch-19 M (BioVentures, Murfreesboro, TN), a modified version that includes a biotin linker and an improved sequence to minimize serum matrix effects. Negative controls were carried out using another HER2 mimotope peptide, PINC (PINCTHSCVDLDDKGCPAEQRASPLTSIISK-Ahx-biotin, United Biosystems), in place of Ch-19 M, and using Avastin® from Genentech USA (i.e. Bevacizumab: a humanized IgG1 kappa light chain mAb specific for vascular endothelial growth factor) in lieu of trastuzumab. Pooled human serum (H4522) and peroxidase conjugated, goat anti-human IgG (Fc-specific) antibody (#A0170) were obtained from Sigma Aldrich.

2.5 Surface functionalization

A thermally deposited gold spot on the topside of the calorimeter membrane allowed for attachment of the Ch-19 M peptide and subsequent trastuzumab binding. Streptavidin was passively adsorbed to the Au surface by incubating streptavidin diluted in PBS (20 μg/ml) on the Au surface for 30 min at room temperature in a humidified petri dish (Ebersole et al. 1990). The sensor surface was rinsed and blocked for 15 s with PBS containing 0.2% Tween 20 (PBS-T). The biotinylated HER2 peptide mimetic Ch-19 M was diluted to 3 μM in PBS-T and coupled to the adsorbed streptavidin by incubating for 20 min at room temperature. The sensor was again rinsed with PBS-T.

2.6 Detection of Trastuzumab

Pooled human serum with varying concentrations of trastuzumab (0–100 μg/ml) was diluted 1:4 in PBS-T and allowed to bind for 20 min to Ch-19 M on the gold sensor surface. After a PBS-T wash, a peroxidase conjugated, goat anti-human IgG (Fc-specific) antibody (diluted 1:250 in PBS-T) was applied to the sensor surface for 20 min at room temperature to bind the available trastuzumab. Unbound peroxidase conjugated anti-human IgG antibody was rinsed from the surface with PBS-T and the sensor surface dried with N_2. The reaction chamber was sealed with a glass cover slide and mineral oil to provide a vapor tight seal that allowed the reaction droplet to persist for up to an hour, although most reactions were completed in less than 5 min. 1 nl of PBS was dispensed onto the center of the sensor. After thermal equilibrium was reached, 100 pl of hydrogen peroxide (50 mM - acting as an electron acceptor) and o-phenylenediamine dihydrochloride (OPD) (100 mM - acting as an electron donor) in PBS was injected into the drop to generate a thermal signal. The resulting thermal output from the reaction of H_2O_2 with the bound peroxidase was recorded in LabView until temperature equilibrium was achieved and the time constant was then calculated in MATLAB. Previous data shows that repeated injections of water into the base drop resulted in a signal baseline drop that scaled with the change in surface area of the drop. Therefore the baseline shift after injection was due to predictable changes in the evaporation rate post-injection and can be removed by fitting the raw signal to an exponential equation (Fig. 3a). The heat integral and time constant (τ) of the temperature decay were then computed from the corrected time trace (Fig. 3b). Since the energy released was constant with regard to H_2O_2 concentration, the time needed to consume the substrate was predicted to be dependent upon the concentration and enzyme-kinetics of the peroxidase indirectly coupled to trastuzumab captured on the calorimeter sensor surface. A calibration curve was constructed to allow the calculation of trastuzumab concentration based on the thermal time constant.

3 Results and discussion

3.1 Calorimeter characterization

Heat flow and electrical modeling in COMSOL Multiphysics showed the optimal configuration to be a 28-junction Bi/Ti thermopile with a 525 μm wide Su-8 polymer membrane and a 200 μm wide hot-junction sensing area (Fig. 4a). The core technology of the TELISA system is a microfabricated polymer membrane based microcalorimeter. Standard microfabrication techniques were used to construct the thin film calorimeters on Si substrates with a high device yield of >85%. Devices showed no degradation in performance over time (6 months) with repeated use, provided the membrane was not ruptured. With a 1 nl sample volume, acid-base and laser calibration (Fig. 5) of the calorimeters showed a minimum detectable power of 375 pW/Hz$^{1/2}$, a power sensitivity

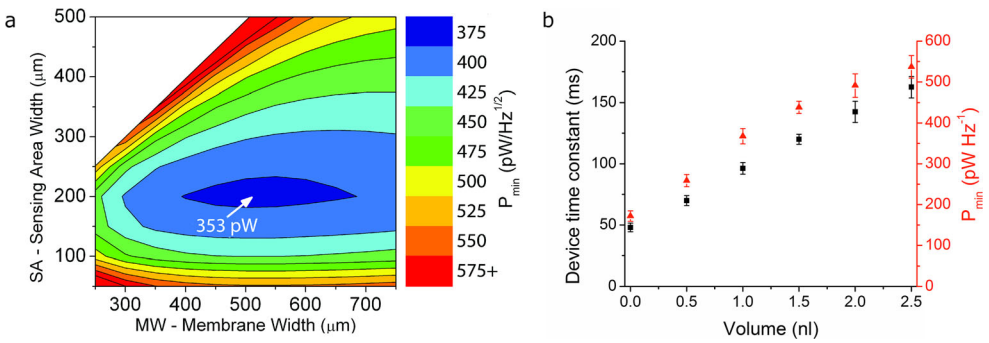

Fig. 4 **a** Calorimeter optimization. Heat flow and electrical modeling in COMSOL and MATLAB were used to determine the optimal dimensions of the calorimeter during the design phase. By balancing thermopile track length, thickness, and membrane size a Pmin of 353 pW/Hz1/2 was predicted. Actual measurements on the constructed calorimeters showed a Pmin of 375 pW/Hz1/2. **b** The microcalorimeter devices have enhances performance at smaller sample volumes. 1 nl was chosen as the optimal volume to balance performance and droplet evaporation. The combination of sub-100 ms time constant and minimum detectable power (Pmin) of 375 nW/√Hz at 1 nl, allows for high resolution measurement of TELISA heat signatures

of 45 *V/W*, and a time constant of 95 ms, all in line with the model predictions (Fig. 4b). This allows for the detection of as little as 4 femtomoles of hydrogen peroxide, or the energy output of 6 attomoles of typical HRP.

3.2 Quantification of Trastuzumab

In the trastuzumab TELISA, it was found that the peroxide reaction time constant (τ) could be varied by changing H_2O_2 concentration, with a shorter τ being obtained at lower concentrations. However, this resulted in a reduced assay signal and an increase in assay background noise. It was determined that a 10 mM concentration of H_2O_2 provided a balance between assay time and signal strength for use in the present application. Trastuzumab concentration and τ correlated well ($R^2 = 0.954$) and that τ could be used to accurately determine trastuzumab concentration in serum to 50 μg/ml (Fig. 5). The limit of detection above baseline noise for the TELISA was 10 μg/ml trastuzumab in human serum. Theraputic serum concentrations of trastuzumab are between 50 to 100 μg/ml, meaning our assay achieves detection and approaches quantification at clinically-relevant levels (Baselga et al. 2005).

Normal human serum contains a high concentration (~9–12 mg/ml serum) of IgG1 antibodies. Normal human serum IgG1 and the negative control humanized therapeutic antibody bevacizumab did not bind to Ch-19 M in the TELISA (Fig. 6). Additionally, trastuzumab in diluted human serum did not bind to the negative control PINC peptide when used in lieu of Ch-19 M. The PINC peptide is another HER2 mimotope, however trastuzumab is known not to bind to it. These results suggest that trastuzumab could be specifically detected in 1 nl of diluted human serum, and that the assay exhibited high sensitivity.

Components (e.g. proteins, lipids, etc.) present in human serum can interfere with antigen (e.g. Ch-19 M) and antibody (e.g. trastuzumab) interactions. These interferences are referred to as serum matrix effects and lead to nonspecific binding. Some serum matrix effects were seen with the TELISA, as signal amplitude was reduced with trastuzumab diluted in human serum rather than PBS buffer (Fig. 7). However, the sensitivity remains constant as demonstrated by the dose response curve (Fig. 6). It will be important to carry out future studies to identify the origin of these serum matrix effects to improve sensitivity.

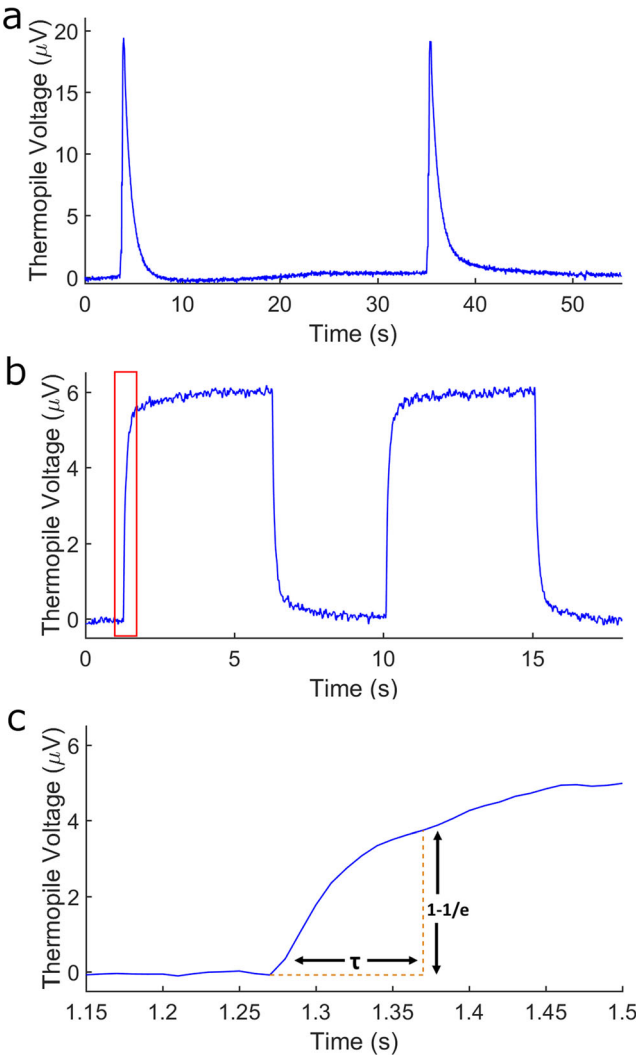

Fig. 5 Calorimeter characterization (**a**) Calorimeter sensitivity calculation. 100 pl of 50 mM HCl was injected into a 1 nl drop of 50 mM NaOH. After baseline drift was corrected and heat of injection removed, the area under the curve was divided by the heat of reaction for each injection (280 nJ) to find device sensitivity. **b** The microcalorimeter time constant was measured using a 650 nm laser focused on a 1 nl water drop centered on the sensing area. The laser was pulsed at 0.2 Hz. **c** Zoomed view of calorimeter response (red box in b). The 1–1/e rise time of the signal was used to determine the sensor time constant

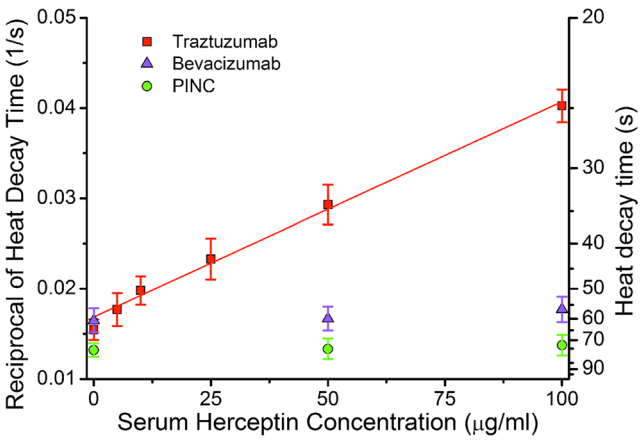

Fig. 6 Trastuzumab dose response. As trastuzumab concentration increases, peroxide is consumed faster; leading to a shorter heat decay time. Negative controls with bevacizumab and PINC show no sensitivity to trastuzumab. The therapeutic dosage of trastuzumab (10–100 μg/ml serum concentration) is well covered by TELISA quantification and is highly correlated to τ (R2 = 0.954). Means ± s.d. are shown ($n = 4$ per point)

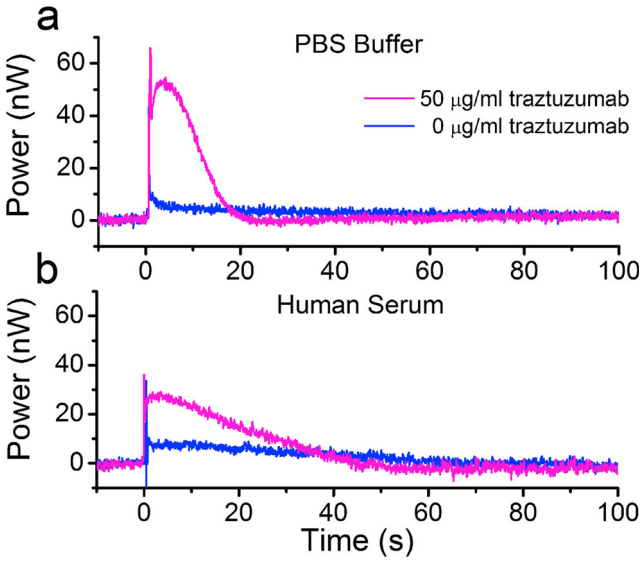

Fig. 7 TELISA signal in PBS and serum (**a**) A strong signal is produced during the detection of 50 μg/ml trastuzumab in PBS. **b** Trastuzumab suspended in human serum shows a lower binding efficiency and a slightly higher background signal - presumably due to serum matrix effects

4 Conclusions

TELISA does not rely on specific reagents and can be widely adapted to a broad spectrum of immunoassays using existing reagents. The thermal signature is quantified using micromachined microcalorimeters with nanoliter sized reaction volumes, sub-nanojoule sensitives, and sub-second time constants. The technology lends itself to a point of care device for high throughput multiplexed assay based on a finger prick. We are currently working on label free point of care systems based on the thermal detection of direct binding events and analyte reactions.

Acknowledgements This work was supported by funding from Vanderbilt University.

References

J. Baselga, X. Carbonell, N.-J. Castañeda-Soto, M. Clemens, M. Green, V. Harvey, et al., Phase II study of efficacy, safety, and pharmacokinetics of Trastuzumab monotherapy administered on a 3-weekly schedule. J. Clin. Oncol. **23**(10), 2162–2171 (2005)

A. Boyer, E. Cissé, Properties of thin film thermoelectric materials: Application to sensors using the Seebeck effect. Mater. Sci. Eng. B **13**(2), 103–111 (1992)

V.H. Carreto-Vazquez, Y.-S. Liu, D.B. Bukur, M.S. Mannan, Chip-scale calorimeters: Potential uses in chemical engineering. J. Loss Prev. Process Ind. **24**(1), 34–42 (2011)

P.J. Delves, I.M. Roitt, *Roitt's Essential Immunology*, 12th edn. (Wiley-Blackwell, Hoboeken, 2011)

E.V. Dolgova, E.A. Alyamkina, Y.R. Efremov, V.P. Nikolin, N.A. Popova, T.V. Tyrinova, et al., Identification of cancer stem cells and a strategy for their elimination. Cancer Biol. Ther. **15**(10), 1378–1394 (2014)

R.C. Ebersole, J.A. Miller, J.R. Moran, M.D. Ward, Spontaneously formed functionally active avidin monolayers on metal surfaces: A strategy for immobilizing biological reagents and design of piezoelectric biosensors. J. Am. Chem. Soc. **112**(8), 3239–3241 (1990)

F.J. Esteva, V. Valero, D. Booser, L.T. Guerra, J.L. Murray, L. Pusztai, et al., Phase II study of weekly docetaxel and Trastuzumab for patients with HER-2–overexpressing metastatic breast Cancer. J. Clin. Oncol. **20**(7), 1800–1808 (2002)

X. Feng, Y. Jia, H. Jiang, Q. Lin, Microfabrication-based isothermal titration calorimetry using a combined in-mixing and post-mixing titration approach. Anal. Methods **10**, 4665–4670 (2018)

B. Jiang, W. Liu, H. Qu, L. Meng, S. Song, T. Ouyand, et al., A novel peptide isolated from a phage display peptide library with Trastuzumab can mimic antigen epitope of HER-2. J. Biol. Chem. **280**(6), 4656–4662 (2005)

E.A. Johannessen, J.M. Weaver, P.H. Cobbold, J.M. Cooper, A suspended membrane nanocalorimeter for ultralow volume bioanalysis. IEEE Trans Nanobioscience **99**(1), 29–36 (2002)

Y. Kudo, M. Nishiwaki, Y. Inoue, N. Seino, T. Nakagama, K. Uchiyama, Rapid ELISA in droplet on PDMS dimple with Nanoliter reagents dispensed by ink-jet microchip. Chem. Lett. **37**(5), 536–537 (2008)

F. Lammers, T. Scheper, in *Thermal Biosensors, Bioactivity, Bioaffinitty.* Thermal biosensors in biotechnology (Springer, Berlin Heidelberg, 1999), pp. 35–67

W. Lee, W. Fon, B.W. Axelrod, M.L. Roukes, High-sensitivity microfluidic calorimeters for biological and chemical applications. Proc. Natl. Acad. Sci. **106**(36), 15225–15230 (2009)

B. Lubbers, Nano-Calorimetry for Point of Care Diagnostics. PhD thesis, Vanderbilt University, Nashville, TN, USA (2015)

B. Lubbers, F. Baudenbacher, Isothermal titration calorimetry in Nanoliter droplets with subsecond time constants. Anal. Chem. **83**(20), 7955–7961 (2011)

B. Mattiasson, C. Borrebaeck, B. Sanfrindson, K. Mosbach, Thermometric enzyme linked immunosorbent assay: TELISA. Biochimica et Biophysica Acta (BBA)-Enzymology **483**(2), 221–227 (1977)

A. Morell, F. Skvaril, E. van Loghem, M. Kleemola, Human IgG subclasses in maternal and fetal serum. Vox Sang. **21**(6), 481–492 (1971)

A.H. Ng, U. Uddayasankar, A.R. Wheeler, Immunoassays in microfluidic systems. Anal. Bioanal. Chem. **397**(3), 991–1007 (2010)

C. Piggee, *In vivo* molecular imaging by LAESI MS. Anal. Chem. **80**(13), 4783 (2008)

P.R. Pohlmann, I.A. Mayer, R. Mernaugh, Resistance to Trastuzumab in breast Cancer. Clin. Cancer Res. **15**(24), 7479–7491 (2009)

S. Premjeet, G. Deepika, B. Sudeep, J. Sonam, K. Sahil, R. Devashish, et al., Enzyme-linked Immuno-sorbent assay (ELISA), basics and it's application: A comprehensive review. J. Pharm. Res. **4**(12), 4581–4583 (2011)

Y. Shang, R. Mernaugh, X. Zeng, Characterization of the native and denatured Herceptin by enzyme linked immunosorbent assay and quartz crystal microbalance using a high-affinity single chain fragment variable recombinant antibody. Anal. Chem. **84**(19), 8164–8170 (2012)

K. Verhaegen, K. Baert, J. Simaels, W. Van Driessche, A high-throughput silicon microphysiometer. Sensors Actuators A Phys. **82**(1), 186–190 (2000)

S. Wang, S. Yu, M. Siedler, P.M. Ihnat, D.I. Filoti, M. Lu, L. Zou, A power compensated differential scanning calorimeter for protein stability characterization. Sensors Actuators B Chem. **256**, 946–952 (2017)